

Effective Hamiltonian approach to kinetic Ising models: Application to an infinitely long-range Husimi-Temperley model

V. I. Tokar

*G. V. Kurdyumov Institute for Metal Physics of the N.A.S. of Ukraine,
36 Acad. Vernadsky Boulevard, UA-03142 Kyiv, Ukraine and
Université de Strasbourg, CNRS, IPCMS, UMR 7504, F-67000 Strasbourg, France*

(Dated: June 15, 2025)

The probability distribution (PD) of spin configurations in kinetic Ising models has been cast in the form of the canonical Boltzmann PD with a time-dependent effective Hamiltonian (EH). It has been argued that in systems with extensive energy EH depends linearly on the number of spins N leading to the exponential dependence of PD on the system size. In macroscopic systems the argument of the exponential function may reach values of the order of the Avogadro number which is impossible to deal with computationally, thus making unusable the linear master equation (ME) governing the PD evolution. To overcome the difficulty, it has been suggested to use instead the nonlinear ME (NLME) for the EH density per spin. It has been shown that in spatially homogeneous systems NLME contains only terms of order unity even in the thermodynamic limit.

The approach has been illustrated with the kinetic Husimi-Temperley model (HTM) evolving under the Glauber dynamics. At finite N the known numerical results has been reproduced and extended to broader parameter ranges. In the thermodynamic limit an exact nonlinear partial differential equation of the Hamilton-Jacobi type for EH has been derived. It has been shown that the average magnetization in HTM evolves according to the conventional kinetic mean field equation.

I. INTRODUCTION

The equilibrium statistics of Ising-type models at a fixed temperature can be described by the canonical probability distribution (CPD) [1]. The latter depends only on the spin configuration energy which is conventionally called the Hamiltonian. CPD is proportional to the Boltzmann factor which is the exponential function of the Hamiltonian divided by $-k_B T$ —the absolute temperature in energy units with the minus sign. In models with short-range interactions the energy scales linearly with the system size N . So if exact analytic solution is unknown, the straightforward use of CPD in approximate calculations would necessitate numerical calculation of the exponential function with the argument scaling as $O(N)$ which can be difficult or even impossible for large N that are of main interest in statistical physics. To deal with this problem, sophisticated combinatorial techniques have been developed to calculate physical quantities of interest without resorting to the numerical exponentiation of $O(N)$ numbers and using only $O(1)$ quantities, such as specific magnetization and the energy density per site [1, 2].

From the standpoint of out of equilibrium statistics CPD is a particular case of more general nonequilibrium probability distribution (NPD) which coincides with CPD in thermal equilibrium. This is conveniently formalized in the effective Hamiltonian (EH) approach [3–5] where the dependence of NPD on EH is posited to be the same as that of CPD on the equilibrium Hamiltonian. This is achieved by defining EH as the logarithm of NPD multiplied by $-k_B T$. This trick allows one to use the approximate techniques of equilibrium statistics [1, 2] also in the nonequilibrium case.

This, however, does not fully solve the problem be-

cause unlike the equilibrium case where the Hamiltonian is constant in time and supposed to be known, EH for a system out of equilibrium should be determined separately. In the case of kinetic Ising models (IM) [6–9], EH evolves with time according to the master equation (ME) for NPD [6]. Because NPD depends on EH and N exponentially, the numerical solution of ME for large N encounters the same over- and underflow difficulties as in the statistical averaging. For example, assuming the number of spins $N = 10^4$ the span of NPD values accessible to calculations within quadruple precision arithmetic will be exhausted by absolute values of EH density only slightly exceeding $k_B T$ which would severely restrict calculations at low temperatures. This could be the reason why simulations in Ref. [10] were restricted to systems containing not more than 10000 spins.

In this paper we will deal with kinetic Ising-type models with Glauber dynamics [7] that have been used to describe out of equilibrium kinetics in a wide variety of systems, such as uniaxial magnets, lattice gases, binary alloys, spin glasses, proteins, neural networks, combinatorial optimization, etc. [1, 11–17].

The aim of the present paper is to suggest a modification of ME along the lines of Ref. [3] such that the resulting evolution equation contained exponential functions with $O(1)$ arguments and in the case of homogeneous systems the equation for EH contained only terms of order unity. It will be shown that this can be achieved at the cost of transforming the linear ME into a nonlinear evolution equation (henceforth abbreviated as NLME). Its derivation will be given in Sec. II. NLME for the kinetic Husimi-Temperley model (HTM) (also known as the infinitely long-range Ising-, the mean field- (MF), the Curie-Weiss-, and the Weiss-Ising model [10, 18–21]) evolving under the Glauber dynamics [7] will be derived

in Sec. III. Numerical merits of NLME will be illustrated on the problem of decay of metastable states in HTM. The decay problem was previously investigated in Refs. [10, 18, 19, 22] in the framework of ME, the Fokker-Planck equation, and the Monte Carlo simulations. In Ref. [10] a scaling law for the lifetime of metastable states was suggested and shown to be valid for large absolute values of a scaling parameter. In Secs. IV and VI it will be shown that the use of NLME allows one to extend the testing range of the scaling law as well as the accuracy of the calculated lifetimes of the metastable states by orders of magnitude. In Sec. V it will be shown that NLME for HTM in the thermodynamic limit reduces to a nonlinear differential equation of the first order. Its characteristic equations will be derived and it will be shown that the conventional MF kinetic equation of Refs. [12, 20, 23] describes a characteristic that passes through the minimum of a free energy function. The description of hysteresis with the use of MF equation, however, is inconsistent because it does not predict a vanishing hysteresis loop area at zero frequency of the oscillating external magnetic field [20]. In Sec. VI a way of resolving this difficulty in HTM framework will be suggested which besides purely theoretical interest may be also of practical importance. It will be argued that HTM at finite N exhibits the Néel-type relaxation [24] which is of interest in biomedical applications where the hysteretic behavior of magnetic nanoparticles is of major importance [25]. In concluding Sec. VII a brief summary will be presented and further arguments given to support the suggestion that NLME is a prospective approach to the solution of stochastic models of the Ising type.

II. EFFECTIVE HAMILTONIAN APPROACH TO KINETIC ISING MODELS

For brevity, the set of N Ising spins $\sigma_i = \pm 1$, $i = 1, N$, will be denoted as $\boldsymbol{\sigma} = \{\sigma_i\}$. In the stochastic approach to nonequilibrium kinetics the statistical properties of an out of equilibrium system can be described by the time-dependent NPD $P(\boldsymbol{\sigma}, t)$ which satisfies ME [6]

$$P_t(\boldsymbol{\sigma}, t) = \sum_{\boldsymbol{\sigma}'} [r(\boldsymbol{\sigma}' \rightarrow \boldsymbol{\sigma}, t)P(\boldsymbol{\sigma}', t) - r(\boldsymbol{\sigma} \rightarrow \boldsymbol{\sigma}', t)P(\boldsymbol{\sigma}, t)]. \quad (1)$$

Here and in the following by subscript t we will denote the partial time derivative; the transition rates r in the kinetic IM will be chosen according to Refs. [7, 8] (the “soft” Glauber dynamics [9] can be treated similarly with minor modifications)

$$r(\boldsymbol{\sigma} \rightarrow \boldsymbol{\sigma}', t) = \frac{1}{\tau_0} \frac{e^{-\mathcal{H}^0(\boldsymbol{\sigma}', t)}}{e^{-\mathcal{H}^0(\boldsymbol{\sigma}', t)} + e^{-\mathcal{H}^0(\boldsymbol{\sigma}, t)}}. \quad (2)$$

where $1/\tau_0$ is the rate of transition $\boldsymbol{\sigma} \rightarrow \boldsymbol{\sigma}'$ and the dimensionless Hamiltonian \mathcal{H}^0 is assumed to include the factor $\beta = 1/k_B T$ as a parameter. \mathcal{H}^0 may depend on

time which is necessary, for example, in modeling the hysteresis [20, 26, 27]. The dependence of the Hamiltonian on $\boldsymbol{\sigma}$ can be arbitrary but in this study we will assume that \mathcal{H}^0 is an extensive quantity, that is, it scales linearly with the system size N [1]. In this case the exponential functions in Eq. (2) scale with N as

$$e^{-\mathcal{H}^0(\boldsymbol{\sigma}, t)} = e^{-N u^0(\boldsymbol{\sigma}, t)}, \quad (3)$$

where $u^0 = O(1)$ is the Hamiltonian density per spin. The exponential behavior in Eq. (3) may hinder numerical solution of ME (1) because the terms on the right hand side (rhs) of Eq. (2) will suffer from the problem of numerical over- and underflow at sufficiently large N . However, when the transition $\boldsymbol{\sigma} \rightarrow \boldsymbol{\sigma}'$ is local, this difficulty is easily overcome. Multiplying the numerator and denominator in Eq. (2) by $\exp\{\frac{1}{2}[\mathcal{H}^0(\boldsymbol{\sigma}, t) + \mathcal{H}^0(\boldsymbol{\sigma}', t)]\}$ one arrives at

$$r(\boldsymbol{\sigma} \rightarrow \boldsymbol{\sigma}') = \frac{1}{2\tau_0} \frac{\exp[\frac{1}{2}\Delta\mathcal{H}^0(\boldsymbol{\sigma}, \boldsymbol{\sigma}', t)]}{\cosh[\frac{1}{2}\Delta\mathcal{H}^0(\boldsymbol{\sigma}, \boldsymbol{\sigma}', t)]} \quad (4)$$

where

$$\Delta\mathcal{H}^0(\boldsymbol{\sigma}, \boldsymbol{\sigma}', t) = \mathcal{H}^0(\boldsymbol{\sigma}, t) - \mathcal{H}^0(\boldsymbol{\sigma}', t). \quad (5)$$

In lattice models with local spin interactions the $O(N)$ scaling of \mathcal{H}^0 is a consequence of the summation over N lattice sites. If configurations $\boldsymbol{\sigma}$ and $\boldsymbol{\sigma}'$ differ only locally, then the difference in Eq. (5) in such models vanishes at large distances from the flipping spin so the summation over sites will be spatially restricted leading to $\Delta\mathcal{H}^0 = O(1)$, hence, all terms in Eq. (4) will be of order unity. (The locality will be discussed in more detail below in Sec. II A.)

We note that Eq. (5) is antisymmetric under the exchange of spin arguments so the denominator in Eq. (4) is the same for both terms in Eq. (1). Replacing it by a constant can simplify ME while preserving its qualitative features [3, 20]. In the present paper, however, more complex Glauber prescription (2) will be used for compatibility with the majority of literature on the kinetic HTM (see, e.g., Refs. [10, 26] and references therein).

Another source of the undesirable behavior briefly discussed in the Introduction comes from NPD P which should depend on N similar to CPD because it coincides with it in thermal equilibrium

$$P(\boldsymbol{\sigma}, t)|_{t \rightarrow \infty} \rightarrow P^0(\boldsymbol{\sigma}) = e^{-\mathcal{H}^0(\boldsymbol{\sigma})}/Z \quad (6)$$

where Z is the partition function and \mathcal{H}^0 in Eq. (6) is assumed to be time-independent because otherwise the equilibrium would not be attainable. It is easily checked that P^0 is a stationary solution of Eq. (1) which means that at least for large t NPD P in Eq. (1) behaves similar to P^0 . This can be formalized in the EH approach [3, 5, 12] where by analogy with Eqs. (6) and (3) NPD depends on EH \mathcal{H} as

$$P(\boldsymbol{\sigma}, t) = e^{-\mathcal{H}(\boldsymbol{\sigma}, t)} \equiv e^{-N u(\boldsymbol{\sigma}, t)}, \quad (7)$$

where $\mathcal{H}|_{t \rightarrow \infty} \rightarrow \mathcal{H}^0 + \ln Z$ and u is the EH density. In Eq. (7) it has been assumed that the normalization constant similar to $\ln Z$ is included in \mathcal{H} . This is convenient in many cases because ME (1) preserves normalization so whenever possible the initial $\mathcal{H}(\boldsymbol{\sigma}, t = t_0)$ is reasonable to choose in such a way that $P(t_0)$ in Eq. (7) was easily normalizable. This would eliminate the necessity to calculate an equivalent of the partition function Z at later stages of evolution because in general this is a nontrivial task.

In Ref. [3] a simple way to eliminate the undesirable exponential behavior from ME is suggested which was implemented as follows. Dividing both sides of Eq. (1) by P from Eq. (7) one arrives after trivial rearrangement at the evolution equation for EH

$$\mathcal{H}_t(\boldsymbol{\sigma}, t) = \frac{1}{\tau_0} \sum_{\boldsymbol{\sigma}'} \frac{\exp\left(\frac{1}{2}\Delta\mathcal{H}^0 - \Delta\mathcal{H}\right) - \exp\left(-\frac{1}{2}\Delta\mathcal{H}^0\right)}{2 \cosh\left(\frac{1}{2}\Delta\mathcal{H}^0\right)} \quad (8)$$

where $\Delta\mathcal{H}$ is defined as in Eq. (5) and normally it should be an $O(1)$ quantity (see Sec. IIA). The arguments of deltas in Eq. (8) have been omitted for brevity; they are the same as in Eq. (5). As is seen, all terms on the rhs are $O(1)$ but because of the summation over $\boldsymbol{\sigma}'$ the equation scales linearly with N . Formally, division of both sides by N would make equation $O(1)$ and fully expressed in terms of EH density defined in Eqs. (3) and (7).

Less formal results can be obtained in spatially homogeneous case. Assuming that the sites are arranged in a Bravais lattice, that is, they are all equivalent, an arbitrary site can be chosen as a reference point. Next applying the cluster approach of the equilibrium alloy theory [13, 28] to Eq. (8) the expansion over a complete set of orthonormal polynomials of $\boldsymbol{\sigma}$ can be restricted only to those containing the chosen site. Further, if the interactions in the system are local (see Sec. IIA), then the size of the system of equations to solve can be approximated by a finite system. In practice, in the alloy thermodynamics the number of clusters to keep in the expansion was found to be rather moderate in many cases [29, 30]. The approximation can be justified with the use of a series expansion. More specific discussion of approximate solution of NLME is not possible because it would strongly depend on an arbitrary initial condition and on unspecified number of time-dependent Hamiltonian parameters.

A. Local interactions in EH

Though nonequilibrium case is difficult to analyze in general terms, in simple cases the locality can be proved.

Let us consider the case of IM with time-independent pair interactions

$$\mathcal{H}^0(\boldsymbol{\sigma}) = -\frac{1}{2} \sum_{i, \vec{e}} K_{i, i+\vec{e}} \sigma_i \sigma_{i+\vec{e}} - h \sum_i \sigma_i \quad (9)$$

where $K_{ij} = J_{ij}/k_B T$, J_{ij} being the pair interactions, $h = H/k_B T$, and H is the magnetic field. The second subscript of K in Eq. (9) is represented as the sum of i and of the radius vector \vec{e} of the relative position of site j with respect to i .

For simplicity let us consider Bravais lattices and assume that the Hamiltonian satisfy all lattice symmetries. In this case the pair interactions K_{ij} depend only on the difference of the lattice coordinates $i - j$ so in Eq. (9) for any site i only dependence on the relative coordinate \vec{e} remains. Further, because the absolute value of the Ising spins is unity, the absolute value of summation over \vec{e} in Eq. (9) will be bounded for all i if

$$\sum_{\vec{e}} |K(\vec{e})| = O(1) \quad (10)$$

which is a formal definition of the short range interaction. The summation over i in Eq. (9) of $N O(1)$ terms makes the energy an extensive quantity for any spin configuration. The criteria for multispin interactions to be short range will have a form similar to Eq. (10) only the summation will be carried over several radius vectors. Though vectors \vec{e} in the summation can be arbitrarily long, the interactions are of short range provided the sum is convergent. Under the Glauber dynamics $\boldsymbol{\sigma}$ and $\boldsymbol{\sigma}'$ in Eq. (5) differ only by one spin on one site, say, i , so only those terms in \mathcal{H}^0 in Eq. (9) that contain this spin will contribute to the difference

$$\Delta_i^{\mathcal{H}^0} = -2\sigma_i \sum_{\vec{e}} K(\vec{e}) \sigma_{i+\vec{e}} - 2h\sigma_i \quad (11)$$

which is $O(1)$ quantity due to Eq. (10) (here $\boldsymbol{\sigma}'$ on the rhs in Eq. (5) has been replaced by $\boldsymbol{\sigma}$ using the fact that $\sigma'_i = -\sigma_i$ while all other spins remain unchanged).

Thus, the terms in Eq. (8) with $\Delta\mathcal{H}^0$ will cause no problems in numerical calculations in case of short range interactions. However, $\Delta\mathcal{H}$ in the equation is not straightforward to analyze because EH is not known and should be determined as the solution of NLME. This in general is a difficult task because the initial condition depends in general on 2^N arbitrary parameters. Besides, arbitrary time dependence in \mathcal{H}^0 is possible in the out of equilibrium systems. Therefore, to make the task manageable, let us consider as an example a frequently studied problem [31] of the quench from a disordered phase at high temperature T_0 to a lower temperature T which we assume to be also large. In this case one can use the high temperature expansion in powers of β or, in our notation, in powers of the dimensionless Hamiltonian \mathcal{H}^0 . For simplicity let us set $T_0 = \infty$ which means the initial value of EH $\mathcal{H}(\boldsymbol{\sigma}, t = 0) = 0$. Because $\mathcal{H}^0 = O(\beta)$ and EH varies from zero at $t = 0$ to \mathcal{H}^0 when $t \rightarrow \infty$, it is also an $O(\beta)$ quantity. Omitting for simplicity the external magnetic field ($h = 0$) and expanding Eq. (8) to the first order in Δ 's it can be shown that Eq. (11) summed over i produces $4\mathcal{H}^0$ and similarly for $\Delta\mathcal{H}$ which, as will be shown, has the same spin structure in this order. Now from Eq.

(9) one gets to the first order in β a linear equation

$$\mathcal{H}_t = 2\tau_0^{-1}(\mathcal{H}^0 - \mathcal{H}) \quad (12)$$

which integration gives

$$\mathcal{H}(\boldsymbol{\sigma}, t) = \mathcal{H}^0(\boldsymbol{\sigma})(1 - e^{-2t/\tau_0}). \quad (13)$$

As is seen, in this approximation EH has the same locality properties as the physical Hamiltonian. Because of nonlinearity of Eq. (8), higher orders in β will be more difficult to analyze. Restricting discussion for simplicity to the case of the nearest neighbor (nn) interactions, it is easy to see that, e.g., in the second order in β the squares of the first order \mathcal{H}^0 will introduce the pair interactions in \mathcal{H} of the extent not exceeding the largest distance within the first coordination sphere. Higher order terms in β will introduce even farther neighbor interactions into EH but to any finite order they will remain bounded by some maximum extent, thus retaining the locality when approximation to this order is adequate.

From a practical standpoint more interesting is the quench to temperatures below T_c [31]. Because the high temperature expansion breaks down in this case, the locality of EH can be substantiated at the initial stage of evolution within the region where expansion in time variable t converges. Assuming as above that at $t = 0$ EH vanishes, the coefficient of linear in t term can be found with the use of Eq. (8) as

$$\mathcal{H}_t|_{t=0} = \tau_0^{-1} \sum_i \tanh(\frac{1}{2}\Delta_i^{\mathcal{H}^0}). \quad (14)$$

Because the hyperbolic tangent is an entire function, it can be expanded in powers of the argument at arbitrarily large values of $\mathcal{H}^0 \propto \beta$ at low temperatures where β is large. In the case of nn interactions, only σ_i and the nn spins will enter the expansion which means that interactions in Eq. (14) will extend not further than the diameter of the first coordination sphere. In higher order terms of expansion in t more distant interactions will arise but they will remain short range to any finite order.

Thus, we have shown that the locality of EH holds within the regions of convergence of two series expansions. Arguably, other expansion techniques suitable to specific physical setups can be developed. The convergence cannot always be guaranteed for any of the expansions but from equilibrium statistics we know that the divergence of a series usually signals the appearance of new physical behavior, such as the phase transitions and/or critical phenomena. It may be expected that in the out of equilibrium evolution the singularities in series expansions would also reveal some new physics, such as the dynamic phase transitions [20, 26].

Though EH cannot be experimentally measured, the distribution of spin configurations depends on EH exactly in the same way as the CPD depends on \mathcal{H}^0 by EH definition. Therefore, the cluster interactions that appear in EH during the evolution will influence the correlation functions in exactly the same way as the physical cluster

interactions occurring in the alloy Hamiltonians [13, 28]. The cluster interactions may influence such observable phenomena as the diffusion scattering [32] and all physical quantities that depend on cluster statistics, such as the electrical conductivity. Therefore, some physical insight into out of equilibrium alloys can be gained from the alloy studies in thermal equilibrium [13, 33].

III. APPLICATION TO HTM

The infinitely long range IM which we call HTM is frequently being used to illustrate general concepts of phase transition theory, such as the critical behavior, using as an example a simple exactly solvable case [22]. Besides, because the exact solution exhibits MF behavior, the equilibrium HTM clarifies the physics underlying MF approximations widely used in the analysis of various models (see, e.g., Refs. [12, 16, 34]). A major result of the present study is that the kinetic HTM evolving under the Glauber dynamics can be also exactly solved in the thermodynamic limit, as will be shown below.

A. HTM at thermal equilibrium

In HTM all spin pairs interact with the same strength $-J/N$ so the dimensionless Hamiltonian reads

$$\mathcal{H}^0 = -\frac{\beta J}{2N} \sum_{i,j=1}^N \sigma_i \sigma_j - \beta H \sum_{i=1}^N \sigma_i \quad (15)$$

where summations over i, j are not restricted to nn pairs as in the conventional IM. Because in this case $K(\vec{e}) = \beta J/N$ does not depend on \vec{e} , the sum in Eq. (10) diverges as $O(N)$. However, the divergence is compensated by the factor $1/N$ in K so HTM formally satisfies the locality Eq. (10) despite being long range.

The extensivity of HTM Hamiltonian can be easily seen if represented in terms of the total spin density m [10]

$$M = \sum_{i=1}^N \sigma_i \equiv Nm \quad (16)$$

as

$$\begin{aligned} \mathcal{H}^0 &= -\frac{\beta J}{2N} M^2 - \beta H M \\ &= -N \left[\frac{\beta}{2} m^2 + h m \right] \equiv Nu^0(m). \end{aligned} \quad (17)$$

Here and in the following to simplify notation we choose J as our energy unit $J = 1$ and $h = \beta H$ is the dimensionless external magnetic field.

The equilibrium partition function

$$Z^{eq} = \text{Tr}_{\boldsymbol{\sigma}} e^{-Nu^0(m)} = \sum_{M=-N}^N N C_{(N+M)/2} e^{-Nu^0(m)} \quad (18)$$

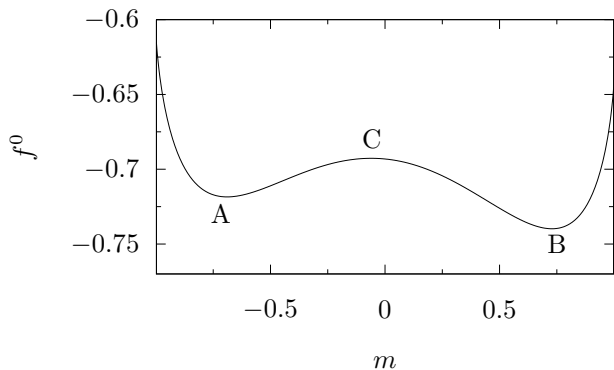


FIG. 1. Equilibrium FFE density Eq. (22) for $T = 0.8T_c$ and $h = 0.015$. A, B, and C denote, respectively, the two local minima and a local maximum appearing in $f^0(m)$ when $T < T_c$ and $|h| < |h_{SP}|$ where h_{SP} is h at the spinodal point (further explanations are given in the text).

where ${}_N C_{(N+M)/2}$ is the combinatorial factor equal to the number of combinations of N spins with magnetization M . In the limit of large N ,—which will be always assumed to be the case in the present study,—the Stirling approximation gives

$$S(N, M) = \ln {}_N C_{(N+M)/2} \simeq Ns(m) \quad (19)$$

with [10, 22]

$$s(m) = - \sum_{\binom{up}{lo}} \frac{1 \pm m}{2} \ln \frac{1 \pm m}{2}. \quad (20)$$

where the sum consists of two terms: one with all lower signs and the other one with all upper signs. Substituting Eq. (20) in Eq. (18) one gets

$$e^{-\beta F^{eq}(h)} \simeq \int_{-1}^1 dm e^{-\beta F^0(m)}, \quad (21)$$

where we have omitted all factors that in the thermodynamic limit do not contribute to $f^0(m)$ defined as [10, 22]

$$\beta F^0(m) \equiv N f^0(m) = N[u^0(m) - s(m)]. \quad (22)$$

We will call F^0 and f^0 the fluctuating free energy (FFE) and FFE density, respectively, because unlike the true free energy they are not convex, as can be seen in Fig. 1 where a typical FFE density for HTM below T_c is drawn. h_{SP} in Fig. 1 and magnetization m_{SP} below in Eq. (62) are the values of h and m at the spinodal point defined by conditions

$$f_m^0 = 0 \text{ and } f_{mm}^0 = 0. \quad (23)$$

Their explicit expressions can be found in Ref. [10]. In Eq. (23) and in the following the subscript m will denote the symmetric discrete derivative defined for an arbitrary function $g(m)$ as

$$g_m(m) = \frac{g(m + \epsilon) - g(m - \epsilon)}{2\epsilon}, \quad (24)$$

where $\epsilon = 1/N$.

As can be seen from Eq. (21) and Fig. 1, in Laplace's approximation suitable at large N only the absolute minimum (or two when $h = 0$) will contribute to f^{eq} while the contributions from the hump in the region of m between points A and B in Fig. 1 will vanish in the thermodynamic limit. However, in nonequilibrium case the behavior of FFE in this region is of paramount importance [10, 26].

B. NLME for HTM

The kinetic HTM has been studied previously within the linear ME and the Fokker-Planck equation approaches in Refs. [10, 18, 19]. Most pertinent to our study will be the numerical data of Ref. [10] so to facilitate comparison we will try to closely follow the notation of that paper.

NLME for HTM can be derived straightforwardly from Eq. (8) using explicit expression for the equilibrium Hamiltonian Eq. (17), allowing the Hamiltonian parameters to depend on time, if necessary. However, to facilitate comparison with Ref. [10], we will derive NLME for HTM departing from Eq. (7) of that reference. To this end we first note that in Ref. [10] the authors considered not individual spins σ_i but the total magnetization M as the fluctuating quantity. Denoting its probability distribution function as $P^{(M)}$ we note that it differs from our P which describes the distribution of the fluctuating Ising spins; in our formulas M serves only as a shorthand for the sum of spins Eq. (16). The configuration space in our case consists of 2^N points while M takes only $N + 1$ values from $-N$ to N with step 2 (a spin flip changes M by 2). This is because many spin configurations correspond to one M value which can be accounted for by the combinatorial factor ${}_N C_{(N+M)/2}$ as

$$P^{(M)}(M, t) = \frac{N!}{N_+! N_-!} P(M, t), \quad (25)$$

where $N_+ = (N + M)/2$ and $N_- = (N - M)/2$ are, respectively, the numbers of spins in the configuration pointing up and down.

In the present notation Eq. (7) of Ref. [10] reads

$$P_t^{(M)}(M, t) = - \frac{1}{2\tau_0} \sum_{\binom{up}{lo}} \left(N_{\pm} \frac{\exp[\mp\beta(M \mp 1)/N \mp h]}{\cosh[\beta(M \mp 1)/N + h]} P^{(M)}(M, t) - (N_{\mp} + 1) \frac{\exp[\pm\beta(M \mp 1)/N \pm h]}{\cosh[\beta(M \mp 1)/N + h]} P^{(M)}(M \mp 2, t) \right), \quad (26)$$

where the summation follows the same rule as in Eq. (20). It should be noted that one of two terms proportional to $P^{(M)}(M \mp 2, t)$ should be set to zero at the end points $M = \pm N$ because values of $|M| > N$ are not allowed.

Now substituting Eqs. (25) and (7) into Eq. (26) one obtains NLME containing only intensive quantities :

$$u_t(m, t) = \frac{1}{4\tau_0} \sum_{\substack{up \\ lo}} (1 \pm m) \left(\frac{\exp[\pm u_m^0(m \mp \epsilon, t)]}{\cosh[u_m^0(m \mp \epsilon, t)]} - \frac{\exp[\mp u_m^0(m \mp \epsilon, t)]}{\cosh[u_m^0(m \mp \epsilon, t)]} e^{\pm 2u_m(m \mp \epsilon, t)} \right). \quad (27)$$

As expected, each term on the rhs of Eq. (27) turns to zero for $u_m(m, t) = u_m^0(m)$ which is a direct consequence of the detailed balance condition satisfied by r in Eq. (2). An important observation is that Eq. (27) contains only derivatives of u with respect to t and m so a constant contribution to EH does not change during the evolution which makes possible normalization of NPD either in the initial condition or at any point during the evolution. It should be noted that no approximations have been made in the derivation, so Eq. (27) is exact. Most importantly, all exponential functions in this equation have arguments of order unity, so their computation is unproblematic for systems of any size.

IV. DECAY OF METASTABLE STATES

Metastable states in many-body systems emerge when there exist local minima in the energy landscape. By definition, they should decay as the system evolves toward thermal equilibrium. The decay process is of paramount importance for the kinetics of phase transitions and has been extensively investigated in a variety of systems [6, 10, 15, 17, 35–38]. In all studies the mechanism of escape from the metastable states was found to proceed via thermal activation with the transition rate depending on the FFE barrier ΔF^* according to the Arrhenius law

$$R \propto \exp(-\Delta F^*/k_B T), \quad (28)$$

where the star denotes the maximum value of the difference between FFE along the reaction pathway and at the local minimum in which the metastable system temporarily resides. The proportionality coefficient in Eq. (28), however, is model-dependent and in the kinetic IM its behavior at low temperatures can be very complicated, as can be seen from analytical calculations and simulations with the use of specialized Monte Carlo algorithms (see Ref. [39] and references therein). The latter approaches were developed to overcome the difficulty encountered in straightforward numerical simulations at low temperatures where the evolution develops at a prohibitively large timescale because of the Arrhenius-law dependence on T .

Apparently for this reason simulations of the decay in HTM in Ref. [10] were restricted to moderately low temperature $T = 0.5T_c$ and to shallow local FFE minima in the vicinity of the spinodal point m_{SP}, h_{SP} defined in Eq. (23). The calculated lifetimes τ of the metastable states were rather modest, $\tau = O(10^4\tau_0)$, so to extend results to larger lifetime values a heuristic asymptotic expression was suggested presumed to be valid for metastable states

($h < h_{SP}$) in the limit

$$|\Lambda| = (h_{SP} - h)N^{2/3} \rightarrow \infty. \quad (29)$$

However, the simulations were performed only for $|\Lambda| \lesssim 4$ [10] and though good agreement with the asymptotic expression was found, it remains unclear whether the data are already in the asymptotic range.

At moderately low temperatures (e.g., $\gtrsim 0.4T_c$ in 2D IM [40]) that will be assumed also in the present paper the qualitative behavior of the decay simplifies and phenomenological classic nucleation theory (CNT) [41] can be used for an accurate calculation of lifetimes in the conventional kinetic IM with nn interactions [36, 38]. CNT, however, is not suitable to deal with HTM because it heavily relies on the short range nature of spin interactions. It is pertinent to note that nucleation time is usually much larger than the time of the subsequent growth of the stable phase, so in most cases the total lifetime of a metastable state τ is dominated by the nucleation time $\tau \simeq 1/R$ which will be assumed throughout the paper.

To understand the difference between nucleation in IM and in HTM, let us consider a ferromagnetic model with Hamiltonian Eq. (9) in equilibrium ordered state below T_c with, say, negative magnetization. The Hamiltonian can describe both IM and HTM by restricting interactions J_{nn} only to nn spins in the former case (here for clarity we temporarily return to dimensional parameters) while in the latter case the interaction is J/N for any spin separation. In both cases the decay is driven by the external field which contribution to FFE difference in Eq. (28) is negative $\sim -2Hs$, where s is the number of reversed spins within the nucleus and FFE at low temperatures is approximated by the interaction energy. The decay is hampered by the positive contribution due to interaction of spins within the nucleus with oppositely directed spins in the bulk. In IM case the nucleus can be chosen to be roughly spherical to minimize the surface where the positive energy density is concentrated so their contribution will scale with s as $cs^{1-1/d}$ where c is a size-independent positive coefficient and d the space dimension [36, 38]

$$\Delta F_{IM} \simeq cs^{1-1/d} - 2Hs. \quad (30)$$

In HTM, however, the positive contribution is not spatially localized because of the infinite range of the interactions so any s spins can be considered as a nucleus (rather a misnomer in this case). Substituting in Eq. (17) $M \simeq -N$ for the metastable system at low temperature $T \rightarrow 0$ and $M \simeq -N + 2s$ for the system with the nucleus one gets after subtraction

$$\Delta F_{HTM} \simeq 2J(1 - s/N)s - 2Hs. \quad (31)$$

The maximum values of the difference needed in Eq. (28) are found from the condition

$$d(\Delta F)/ds|_{s^*} = 0 \quad (32)$$

where s^* is the size of the critical nucleus.

In the case of HTM one finds

$$s^* = \frac{J - H}{2J} N \quad (33)$$

$$\Delta F_{HTM}^* = \frac{(J - H)^2}{2J} N. \quad (34)$$

These expressions qualitatively differ from those that can be obtained from Eq. (30) [36, 38] in that they both linearly depend on N which, in particular, means that in thermodynamic limit the decay is impossible according to Eq. (28). In the IM case, on the other hand, both quantities remain finite as $N \rightarrow \infty$.

The absence of spatial separation between spins with different orientations and the linear dependence of ΔF_{HTM}^* on the system size makes the decay in HTM qualitatively similar to the Néel relaxation in single-domain magnets which will be further discussed below in Sec. VI B.

One may note that Eq. (33) does not make sense for $H > H_c = J$. The reason is that in both HTM and IM there exist some critical value of $H = H_c$ above which the metastability is impossible because the necessary local minimum disappears. As can be seen from Eqs. (4) and (11) the spin flip rate becomes large $\sim \tau_0^{-1}$ irrespective of the spin configuration so spins at random positions can flip to positive values and the system will reach equilibrium on a microscopic time scale $O(\tau_0)$. $H_c = J$ for HTM was obtained in the low temperature approximation; the exact value accounting for entropy effects is H_{SP} [10] and in IM $H_c \simeq H_{SP}$ in MF approximation.

A. The decay in HTM

Because in the thermodynamic limit the decay is impossible in HTM, it has been simulated with the use of NLME at finite N . In HTM the metastable state can form when of $0 \leq h < h_{SP}$ in the vicinity of minimum A in Fig. 1. This problem was investigated in Ref. [10] within linear ME. Following that study the initial condition has been chosen as the Gaussian NPD

$$P^{(M)}(Nm, t = 0) = \sqrt{\frac{aN}{2\pi}} \exp\left[-\frac{aN}{2}(m - m_A)^2\right]. \quad (35)$$

The initial condition for u needed in Eq. (27) has been obtained from an approximate equation

$$P^{(M)}(M, t) \simeq e^{-Nf(m,t)} \quad (36)$$

where in complete analogy with Eq. (22)

$$f(m, t) = u(m, t) - s(m). \quad (37)$$

The approximation for $u(m, t = 0)$ obtained from the last three equations consists in using Stirling's formula for the combinatorial factor in Eq. (25). This is admissible in the case of sufficiently deep metastable minima for large N that we are going to consider because the initial condition can be arbitrary so the slight difference with Ref. [10] is not essential, as discussed in detail below.

In all calculations parameter a in Eq. (35) has been fixed at the same arbitrarily chosen value $a = 1$. Obviously that in general the initial value should strongly influence the outcome of the evolution. However, in our case this will not be significant for the following reason. As was pointed out in Refs. [10, 18, 19], the problem of decay of a metastable state in HTM is akin to the problem of escape over the potential barrier in a two-well potential studied by Kramers [42]. In Ref. [35] the decay is described as follows. At the first stage an arbitrary initial NPD relaxes toward a local quasi-equilibrium state and on the second stage this state slowly (in comparison with the first stage) decays into the stable equilibrium with the magnetic momenta distributed mainly around point B in Fig. 1. In the present study the lifetime τ has been determined at this second stage in contrast to Ref. [10] where the first stage was also included. Because in our definition the properties of both the minima and the Glauber rates depend only on the parameters of HTM, lifetime τ does not depend on arbitrariness of the initial distribution. Now defining the population of metastable state as the number of systems with negative magnetization we may describe its time evolution following Kramers' two-state transition state theory (see Sec. II.C.2 in Ref. [35]) as

$$n_A(t) = \int_{-1}^0 P^{(M)}(Nm, t) dm \simeq n_A^{eq} + (n_A^0 - n_A^{eq})e^{-t/\tau}, \quad (38)$$

where n_A^0, n_A^{eq} are the populations at $t = 0$ and at thermal equilibrium, respectively. The difference with Ref. [10] is that in the present study the behavior Eq. (38) has been assumed to hold only after the initial relaxation has completed while in Ref. [10] it was considered to be approximately valid throughout the whole decay process. In view of this difference, the comparison of our lifetime τ with the calculations of Ref. [10] would be legitimate only if the initial fast relaxation time is negligible in comparison with τ . This has been achieved by restricting consideration to sufficiently deep potential wells near the local minimum A which can be easily satisfied in large systems $N \geq 1000$ where the depth of even a shallow well in f^0 in Fig. 1 is strongly enhanced by the factor N in the expressions of the Arrhenius type satisfied by the lifetime in HTM [10, 18, 19, 42]

$$\tau \sim e^{N[f^0(C) - f^0(A)]} \equiv e^{N\Delta f^0} \quad (39)$$

(we remind that β enters in f^0 as a factor). For example, for the HTM parameters used in the calculations shown in Fig. 2 $n_A^{(eq)} \approx 10^{-38}$. Because of this, the equilibrium population was negligible in the simulations of Ref. [10]

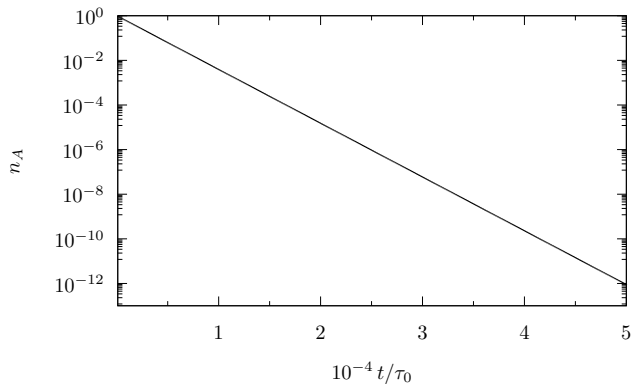


FIG. 2. Probability of survival of the metastable states Eq. (38) calculated with the use of Eq. (27) for HTM with $N = 10^3$, $T = 0.8T_c$, and $h = 0.06$. The points are spaced with time step $100\tau_0$ and their size exceeds the accuracy of calculations. The exponential law has been fulfilled better than the accuracy of the drawing (see the text).

so the authors used Eq. (38) with $n_A^{eq} = 0$. This has been a good approximation also in all calculations of present paper except at $h = 0$ when $n_A^{eq} = n_B^{eq} = 1/2$ due to the symmetry of f^0 in this case (see Fig. 1). The qualitative picture just described is illustrated in Fig. 2 where it can be seen that the decay law Eq. (38) is satisfied at least within twelve orders of magnitude. The influence of the initial relaxation could not be discerned at the time resolution $100\tau_0$. It is to be noted that the lifetime τ in Fig. 2 is only the second smallest in all of our calculations so the influence of the initial relaxation in most of them has been even weaker.

Though the decay law Eq. (38) is only heuristic, in the calculations it has been satisfied with a remarkable accuracy. The specific decay rate

$$\lambda = \tau^{-1}/N \quad (40)$$

has been found to be equal to $5.550091955(7) \times 10^{-7}$ at $t = 200\tau_0, 300\tau_0, 400\tau_0, 500\tau_0$, and $5 \cdot 10^4\tau_0$, that is, it had the same value to the accuracy in nine to ten significant digits.

The simplicity of the behavior seen in Fig. 2 suggests a simple underlying physics which can be surmised from the behavior of FFE during the decay shown in Fig. 3. As can be seen, at intermediate times ($t = 500\tau_0$ has been chosen as an example) $f(m, t)$ in the vicinity of local minima A and B in Fig. 1 can be accurately approximated as

$$f(m, t) \approx f^0(m) + C_{A(B)}(t). \quad (41)$$

In terms of NPD this translates into two quasi-equilibrium distributions strongly peaked near A and B and characterized by filling factors $n_A(t)$ and $n_B(t) = 1 - n_A(t)$ from Eq. (38). The EH density u and FFE f differ only in time-independent function $s(m)$, therefore, large lifetimes of the metastable states means a slow

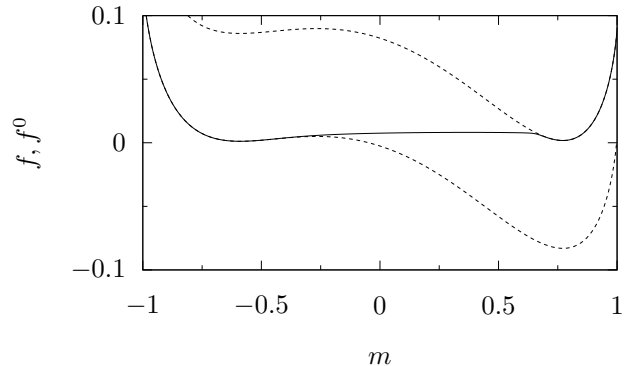


FIG. 3. Solid line—FFE f corresponding to the solution of Eq. (27) at $t = 500\tau_0$ when $n_A \approx n_B$ with the model parameters $\beta = 1.25$ ($T = 0.8T_c$) and $h = 0.06$ with the initial condition Eqs. (35)–(36); dashed lines correspond to local fits of f^0 in Eq. (41).

evolution of both. The behavior of f in Fig. 3 near the minima is easily understood because Eq. (27) has a static solution $u = u^0 + C_0$ where the constant comes from the fact that only derivatives of u with respect to t and m are present in the equation. When $u = u^0 + C_0$ holds for all m , C_0 is fixed by the normalization condition as $C_0 = \ln Z$. But when the equality is only local, as in the figure,—both minima contribute to the normalization via C_A and C_B in Eq. (41).

Still, the cause of the quasi-static behavior of the roughly horizontal line that connects the two regions near the minima in Fig. 3 needs clarification. The qualitative analysis simplifies in the thermodynamic limit where one of the parameters (N) disappears from NLME and its solutions simplify because the escape over barrier is forbidden.

V. THERMODYNAMIC LIMIT AND THE MF EQUATION

For our purposes in taking the limit $N \rightarrow \infty$ in NLME it is convenient, besides setting $\epsilon = 0$, to interchange in Eq. (27) the second terms in the sum over the upper and the lower signs as

$$u_t(m, t) = \frac{1}{4} \sum_{\substack{up \\ lo}} \frac{e^{\pm[u_m^0(m, t) - u_m(m, t)]}}{\cosh u_m^0(m, t)} \left[e^{\pm u_m(m, t)} (1 \pm m) - e^{\mp u_m(m, t)} (1 \mp m) \right] \quad (42)$$

where use has been made of the explicit form of u^0 Eq. (17); besides, henceforth we will choose τ_0 as our time unit and will omit it in evolution equations.

Now it is easily seen that the terms in large brackets in Eq. (42) are nullified by

$$u_m = -\frac{1}{2} \ln \frac{1+m}{1-m} = -\operatorname{artanh} m = s_m(m) \equiv u_m^1 \quad (43)$$

where the penultimate equality follows from Eq. (20). Thus, there exists a locally stationary solution independent of the Hamiltonian parameters which in terms of FFE reads

$$f^1(m) = C_1 \quad (44)$$

where C_1 as a constant. Further, after some rearrangement Eq. (42) takes the form

$$u_t = \cosh^2 u_m (m + \tanh u_m)(\tanh u_m^0 - \tanh u_m) \quad (45)$$

where for brevity the arguments (m, t) of all functions have been omitted. As is seen, if u^0 is time-independent the locally stationary solution satisfying $u_t(m, t) = 0$ is given either by $u = u^0 + \text{Const}$ due to the last factor on the rhs or by u^1 Eq. (43) because of the second factor.

Now the structure of f seen in Fig. 3 becomes qualitatively transparent. In the thermodynamic limit the two segments of f near the minima are given by Eq. (41) with the approximate equality becoming exact and with time-independent $C_{A(B)}$, $n_{A(B)}$ remaining unchanged with time because of the infinitely high barrier separating the minima. At finite but sufficiently large N the solution becomes weakly time-dependent but the qualitative picture remains accurate at large N .

In the Kramers approach to escape over the potential barrier a crucial role plays the diffusivity which is proportional to $\epsilon = 1/N$ [10, 18, 19, 42] and thus can be neglected when the system is very large or the processes studied, such as the high-frequency hysteresis [20, 26, 27], are fast in comparison with the lifetime of metastable states. In such cases the simple Eq. (45) should be easier to use than the system of equations (27) which may become unmanageable at large N . However, the method of solution of Eq. (45) should be chosen prudently. The problem is that numerical techniques are often based on a finite difference approximation of the derivative over m consisting in division of interval $m \in [-1, 1]$ into, say, L discretization steps. In the case of large systems (e.g., $N \sim 10^{23}$) L will be much smaller than N . This would effectively reduce the system size to $\sim L$ which may introduce a nonphysical time evolution, such as the decay of metastable states. A method of characteristics is devoid of such difficulties [43, 44]. The characteristic equations for Eq. (45) has been derived in Appendix A.

A. MF equation

In the Stirling approximation Eq. (25) can be written as

$$P^{(M)}(M, t) \simeq e^{-N[u(m, t) - s(m)]} = e^{-Nf(m, t)}. \quad (46)$$

When $h \neq 0$ the symmetry $m \rightleftharpoons -m$ is broken so in general case there is only one global minimum in $f(m, t)$ at some $m_0(t)$ which can be found from the condition

$$f_m(m, t)|_{m=m_0(t)} = (u_m + \operatorname{artanh} m)|_{m=m_0} = 0 \quad (47)$$

where use has been made of Eqs. (37) and (20). For our purposes the condition is convenient to cast in the form

$$(m + \tanh u_m)|_{m=m_0} = 0 \quad (48)$$

which in terms of the canonical variables of Appendix A can be written as a constraint

$$\chi(m, q) = m + \tanh q = 0. \quad (49)$$

Assuming the FFE minimum in the initial condition is at $m_0(t_0)$ the equation for the characteristic passing through this point is obtained from Eqs. (A5), (A3), (17), and (48) as [23]

$$\dot{m}_0 = -m_0 + \tanh[\beta m_0 + h(t)]. \quad (50)$$

It is straightforward to verify that characteristic Eqs. (A6) and (A7) are also satisfied provided constraint Eq. (49) is fulfilled along the characteristic. This is indeed the case because the total time derivative of χ according to Eq. (A4) is

$$\dot{\chi}(m, q) = \{\chi, \mathbf{H}\} \propto \chi(m, q). \quad (51)$$

Thus, Eq. (49) will be fulfilled along the characteristic if, as we have assumed, it is satisfied at the initial point $t = t_0$.

MF Eq. (50) is a closed equation for the average magnetization m_0 which has been widely used in the studies of the hysteretic behavior (see, e.g., [20, 21, 26, 27]). In the context of the present study a useful observation is that in the case of constant h its variables can be separated and a closed-form solution obtained.

Despite being exact, MF equation is insufficient for description of the HTM kinetics in the thermodynamic limit. As we saw in previous section, the initial condition Eq. (35) had only one extremum but during the evolution two new extrema appeared (see Fig. 3). This behavior cannot be described by MF Eq. (50) but is present in Eq. (45), as illustrates the finite- N example. In the thermodynamic limit such a behavior can be illustrated by the problem of coarsening in a binary alloy [31]. In symmetric ($h = 0$) supercritical ($T > T_c$) phase f^0 has one extremum—the minimum at $m_0 = 0$. If quenched to a subcritical temperature $T < T_c$ the system will evolve toward the equilibrium state with f^0 having a doublewell structure with two symmetric minima at A and B

in Fig. 1 with $h = 0$. This evolution can be described by Eq. (45) while MF equation will remain stuck at point C which will turn into a local maximum at the end of the evolution.

Further, as is known, in MF approximation correlations between the fluctuating variables are neglected, the average of the variables product being approximated by the product of average values. However, the correlations carry important information about the system. For example, by taking statistical average of IM Hamiltonian Eq. (9) it is seen that the internal energy can be expressed exactly in terms of the pair correlation function and the spin average. At thermal equilibrium the pair correlation function is directly related to another important characteristic—the magnetic susceptibility.

In kinetic HTM all correlations between the spin variables are contained in the moments of the magnetization

$$\langle m^n(t) \rangle = \int_{-1}^1 m^n P^{(M)}(Nm, t) dm. \quad (52)$$

$m_0(t)$ entering MF Eq. (50) corresponds to moment $n = 1$, the pair correlation is contained in $\langle m^2 \rangle$. As can be seen from Eq. (35), the latter essentially depends on a at least at the early stage of evolution while this parameter is absent in MF equation Eq. (50). Thus, a complete description of the kinetic HTM can be reached only with the use of FFE $f(m, t)$ satisfying Eq. (45).

VI. LIFETIMES OF METASTABLE STATES

Straightforward calculation of lifetime τ via solution of NLME Eq. (27) and the fit to Eq. (38) has been performed for HTM of two sizes $N = 10^3$ and $2 \cdot 10^3$, two temperatures $T = 0.5T_c$ and $0.8T_c$, and variety of $0 \leq h < h_{SP}$ values. The results are shown in Fig. 4 by open symbols. Larger system sizes were not used because to achieve higher accuracy in Eq. (38) the integration over m has been replaced by the sum over the discrete values

$$m = -1 + 2n\epsilon, \quad n = 0, 1, 2, \dots \quad (53)$$

to use the exact combinatorial factor in $P^{(M)}$ Eq. (25). But this necessitated calculation of $N!$ which has been found to be numerically difficult for $N > 2 \cdot 10^3$ cases studied in Ref. [10]. The use of the Stirling approximation would be sufficient from practical standpoint but to substantiate by numerical arguments a heuristic technique developed below in Sec. VIA, high precision calculations were necessary. Though the use of NLME has made possible to extend the range of calculated lifetimes on an order of magnitude in comparison with Ref. [10], the simulation time grew very quickly with τ so determination of much larger values would have required prohibitively long calculations. Therefore, more efficient, though heuristic technique has been developed.

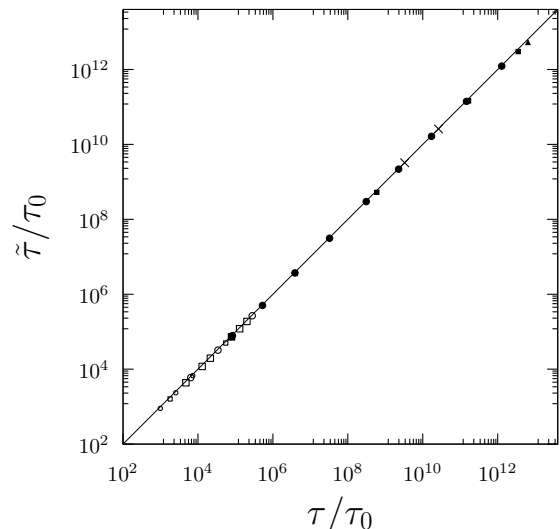


FIG. 4. Comparison of Eq. (62) [10] with lifetimes found from the solution of Eqs. (27) (open symbols) and (56) (filled symbols and crosses). Circles correspond to $T = 0.5T_c$, squares to $T = 0.8T_c$; smaller (larger) symbols correspond to $N = 10^3$ ($N = 2 \cdot 10^3$). The cross at larger (smaller) τ is for $N = 10^5$ ($N = 10^6$); the triangle marks symmetric case $h = 0$ with $N = 10^3$ and $T = 0.8T_c$; the straight line corresponds to $\tilde{\tau} = \tau$. The symbol sizes do not reflect the data accuracy which is higher than the drawing resolution.

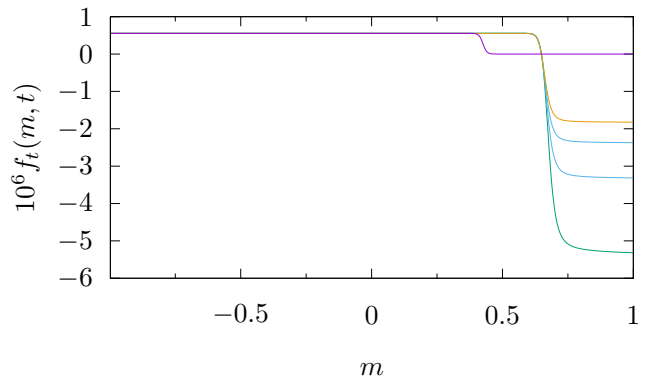


FIG. 5. (Color online) Time derivative of FFE found numerically from Eq. (27) for HTM with the same parameters as in Fig. 2 and for the same five time values of (from bottom to top) as in the text following Eq. (40).

A. Recurrence relation

To clarify the origin of the exponential law Eq. (38) in NLME solutions, let us consider the evolution of FFE shown in Fig. 3 in more detail. We first note that because the configurational entropy Eq. (20) does not depend on time, the time derivative of EH in Eq. (27) is equal to the time derivative of FFE so using the available solution for u the derivative could be calculated numerically, as shown in Fig. 5. As is seen, the time derivative is constant in the region $m \leq 0$ needed in Eq. (38) at all simulated times. Furthermore, it is easy to see that in

this range it should be equal to specific rate λ from Eq. (40) which means that the distribution of m remains the same throughout the evolution and only the total density of metastable states changes with time according to the exponential law Eq. (38). In fact, because the evolution is very slow it is reasonable to expect that the magnetization distribution should be close to the equilibrium one Eq. (6) as illustrated in Fig. 3. In other words, at negative values of m an accurate solution to EH density should be feasible with the *ansatz*

$$u(m, t) \simeq \lambda t + v(m, \lambda). \quad (54)$$

After substitution in Eq. (27) one sees that the time variable disappears from the equation. Also, the two terms in the sum would contain v_m at two successive points $m - \epsilon$ and $m + \epsilon$, so if the leftmost $m = -1$ value is known, the rest can be found successively by recursion [45]. But at $m = -1$ only one term remains on the rhs of Eq. (27), so $v(m = -1 + \epsilon)$ can be expressed through λ and the HTM parameters. Next introducing

$$x_{n+1} = e^{-2[v_m(m+\epsilon) - u_m^0(m+\epsilon)]} - 1, \quad (55)$$

Eq. (27) for x_n can be cast in the form of a nonlinear recurrence relation

$$x_{n+1} = a_n \frac{x_n}{1 + x_n} + b_n \quad (56)$$

where

$$a_n = \frac{1 + m}{1 - m} e^{2u_m^0(m+\epsilon)} \frac{1 + \exp[-2u_m^0(m + \epsilon)]}{1 + \exp[-2u_m^0(m - \epsilon)]} \quad (57)$$

and

$$b_n = -\frac{2\lambda}{1 - m} \left(1 + e^{2u_m^0(m+\epsilon)}\right). \quad (58)$$

(Note that in the above equations only subscript m stands for the discrete derivative, subscripts $n, n + 1$ are just integer numbers.) Thus, from the recurrence relation Eq. (56) all $v(m, \lambda)$ can be found provided a suitable value of λ is chosen in Eq. (58). To understand how this can be done, a more careful analysis of Eqs. (56)–(58) is in order.

To this end we first introduce a useful formal rearrangement of the recurrence. As can be seen from Eq. (57), a_0 is equal to zero so that according to Eq. (56) x_1 is equal to b_0 . Thus, the recurrence can be initiated by x_1 which, as can be seen from Eq. (53), has the lowest physically allowed subscript. However, a simpler solution of the linear recurrence in Appendix B is obtained if it is initiated by $x_0 = 0$ and $a_0 = 1$. This is admissible because for $m = -1$ ($n = 0$) the first term on the rhs of Eq. (56) vanishes, so with $x_0 = 0$ a_0 may be ascribed any value.

A trivial solution of the recurrence is obtained with the choice $\lambda = 0$. Then from Eqs. (56) and (58) follows that $x_n = 0$. According to Eq. (55) this means that $v_m = u_m^0$, that is, the equilibrium solution is recovered. This ought

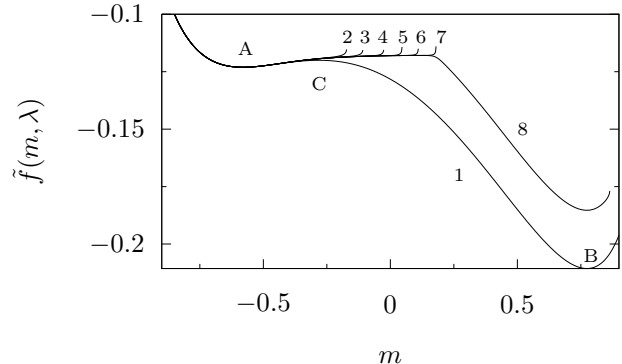


FIG. 6. FFE Eq. (59) calculated with the use of Eqs. (56) and (55) for values of λ given in Table I.

to be expected because $\lambda = 0$ corresponds to a stationary state. Solutions of Eq. (56) will be convenient to visualize with the use of FFE

$$\tilde{f}(m, \lambda) = v(m, \lambda) - s(m). \quad (59)$$

Curve 1 in Fig. 6 corresponds to the fully decayed state (barring the remainder $n_A \sim 10^{-38}$), i.e., to the equilibrium state $v = u^0$. A less trivial solution can be

TABLE I. Values of parameter λ for curves shown in Fig. 6 and the fit of data in Fig. 2 to Eq. (38).

Curve	$10^7 \lambda$
1	0.0
2	6.0
3	5.6
4	5.551
5	5.5501
6	5.550092
7	5.5500919602
8	5.5500919601
Fit	5.55009

obtained for small x_n satisfying

$$\max |x_n| \ll 1 \quad (60)$$

in which case x_n in the denominator in Eq. (56) can be neglected and a closed-form solution obtained (see Appendix B)

$$x_n = \sum_{l=0}^{n-1} b_l \exp \left(\sum_{k=l+1}^{n-1} \ln a_k \right). \quad (61)$$

Using Eq. (58) two immediate conclusions can be made: (i) $x_n \propto \lambda$ and (ii) all x_n for $n \geq 1$ are negative. Thus, when $\max |x_n| \rightarrow 1$ ($x_n \rightarrow -1$) a singularity at $m = -1 + 2n\epsilon$ corresponding to n will arise in x_n , hence, also

in EH and FFE Eq. (59) which means that the solution is unphysical at this value of λ .

Thus, the physical values should be sought in the interval $0 \leq \lambda \leq \lambda_{max}$ with the upper limit found as the largest λ at which the solution does not diverge. This has been done via a trial and error process for the same HTM parameters as in Fig. 2. The results are presented in Fig. 6 and Table I. The range of calculations has been extended beyond $m = 0$ into the region where according to Fig. 5 solution Eq. (54) is still valid. It has been found that $v(m, \lambda)$ is very sensitive to the precise value of λ near λ_{max} . For example, curves 7 and 8 correspond to λ values that differ on a unit in the eleventh significant digit. Yet curve 7 shows that the value is still too large (the solution diverges) while curve 8 already goes deep down and if assumed to be correct predicts $n_A \sim 10^{-27}$, that is the decay is practically terminated. In fact, the curve is drawn farther than the range of validity of Eq. (56) as can be seen by comparing Figs. 5 and 6. But even at the upper end of the region of validity $m \lesssim 0.4$ the value of \tilde{f} is such that $n_A \sim 10^{-10}$. This, however, is an overestimation because the negative derivative of curve 8 indicates that the true value of \tilde{f} near minimum B should be noticeably smaller. Anyway, we are going to compare the calculated lifetimes with those of Ref. [10] defined as the weighted time averages so the contributions of small $n_A(t)$ were insignificant. Thus, in our case a single value of λ_{max} should be sufficient to determine the lifetime from Eq. (40). This is consistent with the data shown in Figs. 2 and 5 where $\lambda \approx 5.55009 \cdot 10^{-7}$ (see Table I) was sufficient to describe the decay from $n_A \approx 0.9$ to 10^{-12} . The agreement of λ found from the recurrence relation with that determined in a fit to the solution of the exact evolution equation to all six significant digits provided by the fitting software supports the suggestion that the heuristic technique based on recurrence Eq. (56) does make possible an accurate determination of lifetimes of the metastable states in HTM. Similar agreement between the two techniques has been found for several other sets of HTM parameters.

The values of τ calculated in this way are shown in Fig. 4 by filled symbols. The excellent agreement with the results of Ref. [10] is illustrated by comparison with the analytic expression suggested in that paper

$$\tilde{\tau} = \frac{\pi}{\sqrt{|m_{SP}|(h_{SP} - h)}} e^{N\Delta f^0}. \quad (62)$$

where Δf^0 has been defined in Eq. (39). In our calculations the notion of scaling in the vicinity of the spinodal has not been used because in some cases, such as the one depicted in Fig. 1, the simulated systems were quite far from it. Therefore, to make comparison with Eq. (41) of Ref. [10] Δf^0 for the barrier height has been used instead of the scaling expression. The comparison with the latter has also been performed with the agreement being only slightly worse than in Fig. 4, arguably, for the above mentioned reason. The upper limit of the data presented in Fig. 4 has been defined by the fact that for the calcula-

tions to be meaningful the second term in the denominator of Eq. (56) $1 + x_n$ should contribute to the recursion from $n = 1$ onward. Therefore, $n_1 = O(\lambda)$ should exceed the smallest number able to change the result when added to unity. In the double precision arithmetic used in calculations it should be larger than $\sim 2 \times 10^{-16}$. The use of software with this quantity being much smaller would make possible to predict much larger lifetimes.

In principle, analytical expression of the type of Eq. (62) should be possible to derive from the condition $x_n \rightarrow -1$. However, this would necessitate knowledge of an analytical expression for x_n which would be difficult to obtain because Eq. (56) becomes strongly nonlinear in this regime.

However, the leading exponential behavior in N can be estimated in the linear approximation Eq. (61). To this end in the expression Eq. (58) for b_n we retain only factor λ , which needs to be found, and in the summation over k only the first two factors in the expression Eq. (57) will be kept because the last factor does not contribute to the logarithm in the limit $\epsilon \rightarrow 0$. With the use of Eq. (20) the first two factors in Eq. (57) can be unified in $\exp[2f_m^0(m_k)]$; here and below m_n, m_l and m_k are connected to n, l, k via Eq. (53). Next, approximating $2 \sum_{l(k)} \approx N \int dm_{l(k)}$ ($dm_{l(k)} \simeq 2/N$) and integrating over dm_k one arrives at an estimate

$$\begin{aligned} \max_n |x_n| &\sim \max_{m_n} \lambda e^{Nf^0(m_n)} \int_{-1}^{m_n} dm_l e^{-Nf^0(m_l)} \\ &\sim \lambda e^{N[f^0(C) - f^0(A)]} \equiv \lambda e^{N\Delta f^0} \simeq 1. \end{aligned} \quad (63)$$

where the integration over m_l for large N has been estimated by Laplace's method, and within the range of validity of Eq. (56) the maximum is attained at $m_n = m_C$. The estimate Eq. (39) now follows from Eq. (40).

The evolution of HTM for $h > h_{SP}$ (in the geometry of Fig. 1) has been found to be not very interesting, mainly because it is not universal as there is no locally stable minimum in f^0 at m_A . The decay of initial state Eq. (35) starts immediately and strongly depends on the arbitrary parameter a . At large $h \gg h_{SP}$ the minimum in f^0 will be moving toward m_B according to MF Eq. (50) in which case the time dependence of n_A will be close to the step function $n_A(t) \approx \theta[-m_0(t)]$. However, in the vicinity of the spinodal when h approaches h_{SP} from above the MF evolution slows down [10] and the diffusion mechanism starts to dominate. The exponential behavior similar to Eq. (38) has been observed for $h \rightarrow h_{SP}^+$ but in the absence of the double-well structure of f^0 its origin is obscure. The second minimum at m_B has been formed which presupposes the existence of the barrier in FFE f $h > h_{SP}$ but whether this kinetically induced shape plays the same role as the double-well structure of equilibrium f^0 is unclear. Besides, when $h > h_{SP}$ the evolution towards thermal equilibrium has been found to be very fast so analytical interpolation to numerically inaccessible regions is not as useful as in the case of escape over high barriers.

To sum up, the techniques developed in the present paper have made possible to substantiate the heuristic expression Eq. (62) for the lifetime of metastable states in HTM suggested in Ref. [10] for about eight orders of magnitude larger values of τ , an order of magnitude larger $|\Lambda| > 20$ in Eq. (29), and for FFE wells farther from the spinodal point up to the symmetric case at zero external field corresponding to the deepest possible well at a given temperature.

B. Néel relaxation and hysteresis

As has been noted earlier, the absence of surfaces separating the regions of differently oriented spins,—hence, no mechanism of domain formation,—as well as the exponential dependence of the metastable lifetimes on the system size makes HTM a viable model of the Néel relaxation (NR) [24] in single-domain magnets with strong uniaxial anisotropy. Additional argument in favor of this possibility gives a common practice to describe NR within the framework of Brown’s discrete orientation model based on the Kramers transition-state theory of escape from the potential well [35, 46, 47] which also successfully describes HTM data, as we saw in Sec. IV A. An advantage of the HTM approach is that unlike in Brown’s description the barrier separating local minima need not be high [46, 47]. The restriction can be detrimental in modeling hysteresis with the external pumping field amplitude exceeding H_{SP} when the energy well becomes shallow or disappears altogether during some time intervals.

Another feature of hysteresis in single-domain magnets that has not yet been satisfactorily described theoretically is that the area of the hysteresis loop should tend to zero in the zero-frequency limit [20, 48]. However, this behavior is not reproduced by MF equations which has been frequently used in hysteresis studies [20, 26, 27]. The MF equation predicts the loop area to be finite at zero frequency which could be attributed to the inadequacy of MF approximation in slowly varying external fields. But as we have shown in Sec. V A, in the thermodynamic limit the average magnetization in HTM satisfies the MF equation exactly which may cast doubt on the soundness of HTM in the description of hysteresis. Apparently, the explanation lies in the fact that in nonequilibrium kinetics the limits $N \rightarrow \infty$ and $t \rightarrow \infty$ are not always interchangeable [49]. In HTM this can be seen from Eq. (38) where the limits $\tau \rightarrow \infty$ and $t \rightarrow \infty$ taken in different order give different results. This problem does not arise in short range IM where τ is finite.

Because the equilibrium can be reached only if τ is finite, in HTM this means finite N . The characteristic time scale separating the two types of behavior is determined by $\tau(h = 0)$ which in the present context can be identified with NR time τ_N . When the period $1/\nu$ (ν is the oscillation frequency) of the external field oscillations is much smaller than τ , the escape over barrier con-

tributes negligibly to the evolution so hysteresis can be described within the MF approach. In the opposite limit $1/\nu \gg \tau$ the system equilibrates by means of escapes. At $h = 0$ the magnetization will be close to zero, as can be seen from Eq. (38) where at $t \rightarrow \infty$ $n_A, n_B \rightarrow 1/2$ the densities of up and down spins will be the same. The response to a weak external field in this case will be that of a paramagnet or, more precisely, of a superparamagnet because the magnetized nanoparticles are not elementary spins and the temperature is below T_c . In the $1/\nu \gg \tau$ and weak external field the magnetic properties can be phenomenologically described within the linear response theory [49, 50].

In recent years, hysteresis and NR in single-domain magnetic nanoparticles attracted much attention in connection with biomedical applications, in particular, in hyperthermia via hysteresis losses [25, 51, 52]. This interdisciplinary technique has many aspects that need be investigated to develop its comprehensive description. The results of the present paper can be useful in qualitatively clarifying a difficulty encountered in the studies of hysteresis which was pointed out in Ref. [52]. Namely, while purely hysteretic behavior for $\tau \gg \nu^{-1}$ and superparamagnetic behavior for $\tau \ll \nu^{-1}$ are covered by existing phenomenological approaches, though only for small amplitudes of the oscillating field in the second case [50], the intermediate regime $\tau \sim \nu^{-1}$ has not yet been satisfactorily described theoretically. But it cannot be avoided in realistic setups because the admissible for biomedical applications nanoparticles have broad size distributions so that the whole region of $\tau(N)$ values may be covered in practice. In the HTM-based approach all frequencies and all field amplitudes can be described within the same formalism, though the problem of very long simulation times needed at large N should be addressed.

VII. CONCLUSION

In this paper a nonlinear master equation (NLME) describing the evolution of the effective Hamiltonian (EH) density has been suggested to overcome the numerical difficulties caused by the exponential dependence of nonequilibrium probability distribution (NPD) that enter into the linear ME [6] on the system size N . In contrast, NLME scales at most as $O(N)$ and can be reduced to a set of $O(1)$ equations in the case of translationally invariant systems.

To illustrate some salient features of NLME in a simple framework, the problem of decay of metastable states in the kinetic Husimi-Temperley model (HTM) has been considered. The problem was previously studied in the framework of linear ME in Refs. [10, 18, 19] which results have been used for comparison purposes. An excellent agreement has been found between numerical NLME solution and the asymptotic analytic expression for the lifetime of metastable states suggested in Ref. [10] for decay in the vicinity of the spinodal. With the use of

NLME it has been possible to cover much broader range of parameters and to achieve much better accuracy. In particular, far from spinodal case of zero external field has been simulated.

The exponential dependence of lifetime on the system size in HTM ensures that in macroscopic systems the lifetime will reach values so large that from physical standpoint the metastable states will behave as effectively stable ones. Because of this, for large N it is reasonable to take thermodynamic limit $N \rightarrow \infty$. It has been shown that in this case NLME simplifies to a nonlinear first-order differential equation possessing, in particular, two locally stable solutions which can be combined to construct stationary EH different from the equilibrium one. To solve the differential equation, a system of characteristic equations has been derived which, in particular, reduces to the conventional MF equation [23] for magnetization corresponding to the fluctuating free energy extrema.

The MF equation that has been widely used in modeling hysteresis [20, 26] was found to fail in the low frequency region [20]. In the present paper it has been shown that at large but finite system size NLME should be able to qualitatively reproduce the correct behavior. Besides purely theoretical interest this should also be useful in modeling Néel relaxation in magnetic nanoparticles which is important in some biomedical applications [25].

An example of NLME application to IM was discussed in Ref. [3]. In a simple pair approximation to EH (which was also used in Ref. [34]) it was found that NLME leads to a qualitatively more sound description of the spinodal decomposition than the MF approximation to ME used, e.g., in Ref. [12]. Specifically, NLME predicted a power-law growth of the volumes of the separating phases while the MF approximation predicts an exponential behavior. The latter is incompatible with the relaxational nature of the stochastic dynamics where the growth exponents cannot be positive [6]. Besides, the characteristic length scale in the MF solution remains constant throughout the growth while NLME predicts a coarse-graining behavior in qualitative agreement with experimental observations.

Switching from a linear ME to the nonlinear equation may seem counterintuitive because the former can be amenable to treatment with the use of powerful techniques of linear algebra. However, they seems to be efficient only when the stochastic matrices are much smaller than the Avogadro number characteristic of the size of macroscopic systems [53]. In statistical physics this case is usually studied in the thermodynamic limit. But NLME has been obtained via substitution of EH into the Boltzmann factor. The subsequent thermodynamic limit has led to a well defined NLME for EH which, however, cannot be linearized back because the corresponding NPD would contain the Boltzmann factor with infinite argument.

The inherently nonlinear nature of ME was also noted in Ref. [6] (see Remark in Ch. V.8) where it was argued that a linear/nonlinear dichotomy is purely mathematical

and does not reflect the underlying physics. For example, the linear Liouville equation is equivalent to Newton's equations which in the case of interacting particles are nonlinear, yet it is the latter that are used in most calculations. Yet another example is given by the BBGKY hierarchy of an infinite number of linear equations which in practical calculations is usually approximated by a finite number of nonlinear ones, such as the Boltzmann transport equation.

These observations may signify that stochastic kinetics in the thermodynamic limit is inherently nonlinear.

ACKNOWLEDGMENTS

I express my gratitude to Hugues Dreyssé for his hospitality, encouragement, and interest in the work. I am grateful to Université de Strasbourg and IPCMS for support.

Appendix A: The Hamilton-Jacobi formalism

Because Eq. (45) contains only derivatives of u but not the function itself, according to Ref. [44] it can be cast in the form of the Hamilton–Jacobi equation [54]

$$u_t + \mathbf{H}(m, q, t) = 0, \quad (\text{A1})$$

where

$$q = u_m(m, t) \quad (\text{A2})$$

and

$$\mathbf{H} = -\cosh^2 q (m + \tanh q) [\tanh u_m^0(m, t) - \tanh q] \quad (\text{A3})$$

is the rhs of Eq. (45) with minus sign. In the Hamiltonian formalism the total time derivative of any function $g(m, q, t)$ of the “coordinate” m and “momentum” q can be calculated as

$$\dot{g} \equiv \frac{dg}{dt} = \frac{\partial g}{\partial t} + \{g, \mathbf{H}\}, \quad (\text{A4})$$

where the Poisson bracket is defined as $\{a, b\} = a_m b_q - a_q b_m$. Now the canonical Hamiltonian equations are easily found as

$$\dot{m} = \mathbf{H}_q \quad (\text{A5})$$

$$\dot{q} = -\mathbf{H}_m. \quad (\text{A6})$$

Further assuming that at some $t = t_0$ an initial Hamiltonian density $u(m, t_0)$ is known, by choosing any admissible value m_0 and setting $q(t_0)$ equal to $u_m(m_0, t_0)$ one can find $m(t)$ and $q(t)$ from the solution of the initial value problem for Eqs. (A5) and (A6). Next integrating equation

$$\dot{u} = q\mathbf{H}_q - \mathbf{H} \quad (\text{A7})$$

obtained from Eqs. (A4), (A5), (A2), and (A1) one arrives at a solution for $u(m, t)$ in parametric form where at each t the values of u at different m are found from the solution of the above initial-value problem for all possible $m_0 = m(t_0)$. Such a solution is a particular case of the general method of characteristics [43].

A rigorous derivation of the Hamiltonian-Jacobi formalism in the general case of many variables can be found in Ref. [44] but for our Eq. (A1) the following heuristic arguments should suffice. First we observe that the partial derivative u_m in Eq. (45) couples the values of function $u(m, t)$ at neighbor points $m \pm \epsilon$ so by using, e.g., the method of lines one should solve a system of $N \rightarrow \infty$ coupled ordinary evolution equations. In the method of characteristics one tries to reduce the problem to only a few such equations. To this end one may observe that by taking the total time derivative of Eq. (A2) in the conventional way one gets

$$\dot{q} = u_{mt} + u_{mm}\dot{m} = -\mathbf{H}_m - \mathbf{H}_q u_{mm} + u_{mm}\dot{m} \quad (\text{A8})$$

where the second equality has been obtained by differentiating Eq. (A1) with respect to m by considering q in \mathbf{H} as just another notation for u_m . Now if we *demand* that Eq. (A5) was satisfied, then Eq. (A6) would follow from Eq. (A8). Eq. (A7) also is easily obtained by differentiating $u(m, t)$, using Eq. (A1) and applying the chain rule. Next assuming $m = m(t)$ on the characteristic line, substituting it in Eqs. (A5), (A6), and (A7) one arrives at a system of three evolution equations for three unknown functions. It is to be noted that Eqs. (A5) and (A6) are sufficient to derive Eq. (A4) which shows the consistency

of our assumptions.

Appendix B: Linear recurrence [45]

Let us consider a linear recurrence relation

$$x_{n+1} = a_n x_n + b_n \quad (\text{B1})$$

initiated by x_0 ; a_n and b_n , $n = 0, N$ are presumed to be known. Now by introducing

$$X_n = \frac{x_n}{\prod_{k=0}^{n-1} a_k} \quad (\text{B2})$$

and dividing both sides of Eq. (B1) by $\prod_{k=0}^n a_k$ one arrives at a linear difference equation

$$X_{n+1} - X_n = b_n / \prod_{k=0}^n a_k \quad (\text{B3})$$

which can be solved as

$$X_n = X_0 + \sum_{l=0}^{n-1} \frac{b_l}{\prod_{k=0}^l a_k}. \quad (\text{B4})$$

In the main text it was assumed that $x_0 = 0$ which in combination with Eq. (B2) gives $X_0 = 0$ and

$$x_n = \sum_{l=0}^{n-1} b_l \prod_{k=l+1 \leq n-1}^{n-1} a_k = \sum_{l=0}^{n-1} b_l \exp \left(\sum_{k=l+1 \leq n-1}^{n-1} \ln a_k \right). \quad (\text{B5})$$

-
- [1] K. Huang, *Statistical mechanics*, 2nd ed. (John Wiley & Sons, Inc., New York, 1987).
- [2] F. Englert, Linked cluster expansions in the statistical theory of ferromagnetism, *Phys. Rev.* **129**, 567 (1963).
- [3] V. I. Tokar, Hamiltonian approach to kinetic Ising models, *Phys. Rev. E* **53**, 1411 (1996).
- [4] V. G. Vaks, Master equation approach to the configurational kinetics of nonequilibrium alloys: exact relations, H-theorem, and cluster approximations, *JETP Lett.* **63**, 471 (1996).
- [5] M. Nastar, V. Dobretsov, and G. Martin, Self-consistent formulation of configurational kinetics close to equilibrium: The phenomenological coefficients for diffusion in crystalline solids, *Phil. Mag. A* **80**, 155 (2000).
- [6] N. G. van Kampen, *Stochastic processes in physics and chemistry* (Elsevier Science B.V., Amsterdam, 1992).
- [7] R. J. Glauber, Time-dependent statistics of the Ising model, *J. Math. Phys.* **4**, 294 (1963).
- [8] K. Kawasaki, Diffusion constants near the critical point for time-dependent Ising models I, *Phys. Rev.* **145**, 224 (1966).
- [9] K. Park, P. A. Rikvold, G. M. Buendía, and M. A. Novotny, Low-temperature nucleation in a kinetic Ising model with soft stochastic dynamics, *Phys. Rev. Lett.* **92**, 015701 (2004).
- [10] T. Mori, S. Miyashita, and P. A. Rikvold, Asymptotic forms and scaling properties of the relaxation time near threshold points in spinodal-type dynamical phase transitions, *Phys. Rev. E* **81**, 011135 (2010).
- [11] Y. Toga, S. Miyashita, A. Sakuma, and T. Miyake, Role of atomic-scale thermal fluctuations in the coercivity, *npj Computational Materials* **6**, 1 (2020).
- [12] J.-F. Gouyet, M. Plapp, W. Dieterich, and P. Maass, Description of far-from-equilibrium processes by mean-field lattice gas models, *Adv. Phys.* **52**, 523 (2003).
- [13] F. Ducastelle, *Order and Phase Stability in Alloys* (North-Holland, Amsterdam, 1991).
- [14] T. Plefka, Modified Thouless-Anderson-Palmer equations for the Sherrington-Kirkpatrick spin glass: Numerical solutions, *Physical Review B* **65**, 224206 (2002).
- [15] P. Bruscolini, A. Pelizzola, and M. Zamparo, Rate determining factors in protein model structures, *Phys. Rev. Lett.* **99**, 038103 (2007).
- [16] M. Aguilera, S. A. Moosavi, and H. Shimazaki, A unifying framework for mean-field theories of asymmetric kinetic Ising systems, *Nature Communications* **12**, 1197 (2021).

- [17] S. Kirkpatrick, C. D. Gelatt, and M. P. Vecchi, Optimization by simulated annealing, *Science* **220**, 671 (1983).
- [18] H. Tomita, A. Itō, and H. Kidachi, Eigenvalue problem of metastability in macrosystem, *Prog. Theo. Phys.* **56**, 786 (1976).
- [19] B. J. Matkowsky, Z. Schuss, C. Knessl, C. Tier, and M. Mangel, Asymptotic solution of the Kramers-Moyal equation and first-passage times for Markov jump processes, *Phys. Rev. A* **29**, 3359 (1984).
- [20] B. K. Chakrabarti and M. Acharyya, Dynamic transitions and hysteresis, *Rev. Mod. Phys.* **71**, 847 (1999).
- [21] G. Carinci, Random hysteresis loops, *Ann. Inst. H. Poincaré Probab. Statist.* **49**, 307 (2013).
- [22] S. Salinas, *Introduction to Statistical Physics*, Graduate Texts in Contemporary Physics (Springer New York, 2001).
- [23] M. Suzuki and R. Kubo, Dynamics of the Ising model near the critical point I, *J. Phys. Soc. Jpn.* **24**, 51 (1968).
- [24] L. Néel, Influence des fluctuations thermiques a l'aimantation des particules ferromagnétiques, *CR Acad. Sci.* **228**, 664 (1949).
- [25] F. Wiekhorst, U. Steinhoff, D. Eberbeck, and L. Trahms, Magnetorelaxometry assisting biomedical applications of magnetic nanoparticles, *Pharm. Res.* **29**, 1189 (2012).
- [26] T. Tomé and M. J. de Oliveira, Dynamic phase transition in the kinetic ising model under a time-dependent oscillating field, *Phys. Rev. A* **41**, 4251 (1990).
- [27] H. Zhu, S. Dong, and J.-M. Liu, Hysteresis loop area of the ising model, *Phys. Rev. B* **70**, 132403 (2004).
- [28] J. Sanchez, F. Ducastelle, and D. Gratias, Generalized cluster description of multicomponent systems, *Physica A* **128**, 334 (1984).
- [29] M. Asta, C. Wolverton, D. de Fontaine, and H. Dreyssé, Effective cluster interactions from cluster-variation formalism. I, *Phys. Rev. B* **44**, 4907 (1991).
- [30] C. Wolverton and A. Zunger, Ni-Au: A testing ground for theories of phase stability, *Comput. Mater. Sci.* **8**, 107 (1997), proceedings of the joint NSF/CNRS Workshop on Alloy Theory.
- [31] L. F. Cugliandolo, Coarsening phenomena, *C. R. Phys.* **16**, 257 (2015).
- [32] I. Masanskii and V. Tokar, Cluster probabilities in binary alloys from diffraction data, *Journal de Physique. I* **2**, 6 (1992).
- [33] I. V. Masanskii, V. I. Tokar, and T. A. Grishchenko, Pair interactions in alloys evaluated from diffuse-scattering data, *Phys. Rev. B* **44**, 4647 (1991).
- [34] M. Nastar, A mean field theory for diffusion in a dilute multi-component alloy: a new model for the effect of solutes on self-diffusion, *Phil. Mag.* **85**, 3767 (2005).
- [35] P. Hänggi, P. Talkner, and M. Borkovec, Reaction-rate theory: fifty years after Kramers, *Rev. Mod. Phys.* **62**, 251 (1990).
- [36] M. Acharyya and D. Stauffer, Nucleation and hysteresis in Ising model: classical theory versus computer simulation, *Eur. Phys. J. B* **5**, 571 (1998).
- [37] H. Nishimori, *Statistical Physics of Spin Glasses and Information Processing: An Introduction*, International series of monographs on physics (Oxford University Press, 2001).
- [38] S. Ryu and W. Cai, Validity of classical nucleation theory for Ising models, *Phys. Rev. E* **81**, 030601 (2010).
- [39] V. A. Shneidman and G. M. Nita, Nucleation preexponential in dynamic Ising models at moderately strong fields, *Phys. Rev. E* **68**, 021605 (2003).
- [40] B. J. Kooi, Cluster evolution in a cold Ising ferromagnet: Disappearance of magic numbers with temperature rise, *Phys. Rev. B* **77**, 024303 (2008).
- [41] R. P. Sear, Nucleation: theory and applications to protein solutions and colloidal suspensions, *J. Phys. Condens. Matter* **19**, 033101 (2007).
- [42] H. A. Kramers, Brownian motion in a field of force and the diffusion model of chemical reactions, *Physica* **7**, 284 (1940).
- [43] G. Whitham, *Linear and Nonlinear Waves*, Pure and Applied Mathematics: A Wiley Series of Texts, Monographs and Tracts (Wiley, 2011).
- [44] E. Kamke, *Differentialgleichungen Lösungsmethoden und Lösungen. Band II: Partielle Differentialgleichungen erster Ordnung für eine gesuchte Funktion* (Akademische Verl. Ges., Leipzig, 1959).
- [45] Wikimedia Foundation, Recurrence relation, https://en.wikipedia.org/wiki/Recurrence_relation (2023), last accessed 08/05/2023.
- [46] W. T. Coffey, P. J. Cregg, and Y. U. P. Kalmykov, On the theory of Debye and Néel relaxation of single domain ferromagnetic particles, in *Advances in Chemical Physics* (John Wiley & Sons, Ltd, 1992) Chap. 5, pp. 263–464.
- [47] P. Ilg, Diffusion-jump model for the combined Brownian and Néel relaxation dynamics of ferrofluids in the presence of external fields and flow, *Phys. Rev. E* **100**, 022608 (2019).
- [48] S. W. Sides, P. A. Rikvold, and M. A. Novotny, Stochastic hysteresis and resonance in a kinetic Ising system, *Phys. Rev. E* **57**, 6512 (1998).
- [49] D. Forster, *Hydrodynamic Fluctuations, Broken Symmetry, and Correlation Functions* (Addison-Wesley, NY, 1983).
- [50] R. Rosensweig, Heating magnetic fluid with alternating magnetic field, *J. Magn. Magn. Mater.* **252**, 370 (2002).
- [51] R. Hergt, S. Dutz, and M. Röder, Effects of size distribution on hysteresis losses of magnetic nanoparticles for hyperthermia, *J. Phys.: Condens. Matter* **20**, 385214 (2008).
- [52] S. Ruta, R. Chantrell, and O. Hovorka, Unified model of hyperthermia via hysteresis heating in systems of interacting magnetic nanoparticles, *Sci. Rep.* **5**, 9090 (2015).
- [53] D. J. Sharpe and D. J. Wales, Nearly reducible finite Markov chains: Theory and algorithms, *J. Chem. Phys.* **155**, 140901 (2021).
- [54] Wikimedia Foundation, Hamilton-Jacobi equation, https://en.wikipedia.org/wiki/Hamilton-Jacobi_equation (2023), last accessed 05/21/2023.